Available online at www.sciencedirect.com
SCIENCE DIRECT®
Biochemical and Biophysical Research Communications 314 (2004) 586–596
BBRC
www.elsevier.com/locate/ybbrc

Sorting pathway and molecular targeting signals for the *Arabidopsis* peroxin 3

Joanne E. Hunt and Richard N. Trelease*

School of Life Sciences, Cellular and Molecular Biosciences, Arizona State University, Tempe, AZ 85287-4501, USA

Received 15 December 2003

Abstract

Peroxin 3 (Pex3p) has been identified and characterized as a peroxisomal membrane protein in yeasts and mammals. We identified two putative homologs in *Arabidopsis* (AtPex3p, forms 1 and 2), both with an identical cluster of positively charged amino acid residues (RKHRRK) immediately preceding one of the two predicted transmembrane domains (TMD1). In transiently transformed *Arabidopsis* and tobacco BY-2 suspension-cultured cells, epitope-tagged AtPex3p (form 2) sorted post-translationally from the cytosol directly to peroxisomes, the first sorting pathway described for any peroxin in plants. TMD1 and RKHRRK were necessary for targeting form 2 to peroxisomes and sufficient for directing chloramphenicol acetyltransferase to peroxisomes in both cell types. The N and C termini of AtPex3p (form 2) extend into the peroxisomal matrix, different from mammal and yeast Pex3 proteins. Thus, two authentic peroxisomal membrane-bound Pex3p homologs possessing a membrane peroxisomal targeting signal, the first one defined for a plant peroxin and for any Pex3p homolog, exist in plant cells.

Keywords: *Arabidopsis*; BY-2; Membrane targeting signal; Pex3p; Peroxin; Peroxisome; Transmembrane domain

Peroxisomes are ubiquitous in cells of eukaryotic organisms, constituting a dynamic class of subcellular organelles. Relatively small in diameter (0.1–1.0 μm) and delineated by a single boundary membrane, peroxisomes do not possess their own nucleic acids; consequently, they are solely dependent on the nuclear genome. In all organisms, peroxisomes function in oxidative metabolism that involves oxidases and elimination of H_2O_2 and reactive oxygen species [1,2]. Peroxisomes also participate in a variety of metabolic pathways depending on the organism, developmental stage, cell/tissue, environment, etc. For example, yeast peroxisomes house inducible enzymes capable of metabolizing alkanes, fatty acids, methanol, uric acid, or primary amines [3]. In mammals, peroxisomes participate in the synthesis of ether-linked phospholipids and sterols, and in the degradation of long chain fatty acids and phytanic acid [4,5]. In higher plants, peroxisomes are subdivided according to their main function into four classes: (a) glyoxysomes in oilseed seedlings house enzymes of the glyoxylate cycle and β-oxidation of fatty acids, (b) leaf-type peroxisomes in photosynthetic tissues contain enzymes that participate in photorespiration, (c) root nodule peroxisomes in differentiated cells of legume nodules possess enzymes essential for ureide biosynthesis, and (d) unspecialized peroxisomes contain the basic enzymes for all peroxisomes, namely catalase and oxidases [6,7].

The most recent focus of peroxisomal research has been the elucidation of biogenetic events related to these organelles [8–10]. Proteins involved in peroxisomal biogenesis are termed peroxins (Pex), most of which are peroxisomal membrane proteins (PMP) [11,12]. Analyses of yeast *PEX* mutants have been instrumental in discovering putative peroxins in mammals, plants, and trypanosomes [13,14]. The importance of identifying and characterizing peroxins is underscored in humans who suffer from peroxisomal biogenesis disorders resulting in lethal diseases such as Zellweger syndrome, X-linked adrenoleukodystrophy, and Refsum disease [15]. These diseases are attributed to missing or aberrant biogenetic peroxins.

* Corresponding author. Fax: 1-480-965-6899.
E-mail address: trelease.dick@asu.edu (R.N. Trelease).

0006-291X/$ - see front matter © 2003 Elsevier Inc. All rights reserved.
doi:10.1016/j.bbrc.2003.12.123

Mature functional peroxisomes house an array of matrix proteins, which possess well-characterized peroxisomal targeting signals (PTSs) [12,16]. They are either a type 1 or type 2 PTS (PTS1 or PTS2), which is recognized by the cytosolic receptors Pex5p and Pex7p, respectively. PTS1 is a carboxy terminal tripeptide composed generally of small-basic-hydrophobic amino acid residues, such as the prototypic serine–lysine–leucine sequence [12,17], whereas PTS2 is a nonapeptide (R/K)(L/V/I)X_5(H/Q)(L/A) found within or at the amino terminus of a different subset of matrix proteins [8,18–20].

Targeting signals for membrane proteins are distinctly different from those directing proteins to the matrix. Transmembrane domain(s) (TMD) flanked on either side by a stretch of basic amino acid residues generally constitute a membrane peroxisomal targeting signal (mPTS) [21,22]. Peroxisomal targeting of PMP47 in the yeast *Candida boidinii* requires multiple elements for targeting to peroxisomes including: (a) a cytosolic orientated loop of amino acid residues between TMD1 and TMD2, (b) the second of five TMDs, (c) a short matrix loop containing basic amino acids, and (d) a membrane anchoring TMD [23,24]. The human counterpart to PMP47, PMP34, contains two non-overlapping sets of targeting information which are composed of amino or carboxy terminal membrane spanning domains and a cluster of basic amino acid residues [25]. Targeting of human PMP22 was similar in that it required two distinct non-overlapping TMDs and corresponding basic polypeptide loops to efficiently target to GFP peroxisomes [26]. Targeting of PMPs in plants is predicted to be analogous to that observed in yeasts and mammals. For example, the *Arabidopsis* PMP22 mPTS is composed of at least four distinct regions within the N-terminal one-half of PMP22 that includes a positively charged domain and all four TMDs [27]. The mPTS of cottonseed peroxisomal ascorbate peroxidase (APX) is composed of its C-terminal TMD and adjacent basic cluster of amino acid residues [28]. An obvious void in the literature are data describing the necessary and sufficient elements of a mPTS for any plant peroxin.

In this study we report that there are two *Arabidopsis* peroxin 3 homologs (AtPex3p, form 1 and form 2), which are unique to the single forms of Pex3p reported for yeasts [29–32] and mammals [33,34]. In vivo immunofluorescence microscopy of transiently expressed proteins was employed to determine the subcellular localization of AtPex3p (form 2) in *Arabidopsis* and tobacco BY-2 suspension-cultured cells. Experimental results revealed that AtPex3p (form 2) sorts directly from the cytosol to peroxisomes in both cell types. Both forms of AtPex3p possess targeting elements similar to those reported for Pex3 proteins in yeasts and mammals, even though the primary amino acid sequence identity of the *Arabidopsis* forms is less than 19–25% of the yeast and mammalian Pex3 proteins. In vivo experimental results also revealed that the topological orientation of AtPex3p form 2 (N_{in}–C_{in}) differs from that of any of the yeast or mammalian Pex3 proteins that have been examined.

Materials and methods

Plasmid constructions. Molecular biology reagents were purchased from Promega (Madison, WI), New England Biolabs (Beverly, MA) or Takara Biomedicals (Otsu, Shiga, Japan). Standard recombinant DNA procedures were used, and whole-plasmid PCR-based mutagenesis reactions were carried out using *QuickChange* Site-Directed Mutagenesis Kit (Stratgene, La Jolla, CA). Oligonucleotide primers were synthesized by Genetech Biosciences (Tempe, AZ) and dye terminator DNA cycle sequencing was done at the Arizona State University DNA facility (Tempe, AZ).

Construction of pRTL2/BXc*myc* was carried out in a two-step process. First, whole-plasmid PCR-based mutagenesis was performed with template pRTL2/n*myc*BX, which has an in-frame *Bam*HI and *Xba*I site followed by a single copy of the *myc*-epitope (donated by Robert Mullen, University of Guelph, Guelph, Ontario, Canada), as template DNA. A forward primer (5′-CTGAAGAAGATCTGTGA AGAGTCCGCAAAAATC-3′) and a reverse primer (5′-GATTTT TGCGGACTCTTCACAGATCTTCTTCAG-3′) introduced a termination codon at the 3′ end of the *myc* coding sequence and deleted *Bam*HI and *Xba*I sites to yield pRTL2/n*myc*ΔBX + UGA. Second, using pRTL2/n*myc*ΔBX + UGA, as template DNA the PCR mixture included a forward primer (5′-CGAACGATAGCCGGATCCTCTAG AGAACAAAAGTTGATTTC-3′) and a reverse primer (5′-GAA ATCAACTTTTGTTCTCTAGAGGATCCGGCTATCGTTCG-3′) that introduced *Bam*HI and *Xba*I sites upstream of the *myc* coding sequence, and deleted the *myc* translation initiation codon to yield pRTL2/BXc*myc*.

An expressed sequence tag (EST) of the *Arabidopsis* gene encoding PEX3 (AtPEX3) (form 2) (pU21561) on chromosome 1 of the Columbia ecotype was obtained from the *Arabidopsis Biological Resource Center* (Ohio State University). There was no available EST clone for AtPEX3 (form 1). The first step in construction of pRTL2/n*myc*-AtPEX3 and pRTL2/c*myc*-AtPEX3 (Table 1) involved PCR amplification of the complete ORF of AtPEX3 (form 2) in pU21561. For construction of pRTL2/n*myc*-AtPEX3, AtPEX3 was PCR amplified with a forward mutagenic primer (5′-CGCGGATCCGATTTCGTT AGGGGTTTTTGG-3′) that replaced the start methionine with an in-frame *Bam*HI site, and a reverse primer (5′-GCTCTAGAGCCT ATTGCGGCATATTAGC-3′) that introduced an in-frame *Xba*I site at the 3′ end of the stop codon. For construction of pRTL2/c*myc*-AtPEX3, a forward primer (5′-CGCGGATCCGCGATGGATTTC GTTAGGGG-3′) that introduced an in-frame *Bam*HI site and a reverse mutagenic primer (5′-CGTCTAGATTGCGGCATATTA GCG-3′) that replaced the termination codon with an in-frame *Xba*I site were used in the PCRs. The resulting PCR products from both reactions were TA-cloned into pCR2.1 (Invitrogen, San Diego, CA), digested with *Bam*HI/*Xba*I, and then ligated into *Bam*HI/*Xba*I-digested pRTL2/n*myc*BX or pRTL2/BXc*myc* to yield pRTL2/n*myc*-AtPEX3 and pRTL2/c*myc*-AtPEX3.

DNA fusion constructs pRTL2/40AtPEX3-CAT, pRTL2/16AtPEX3-CAT, and pRTL2/8AtPEX3-CAT (Table 1) coding for proteins with the N-terminal 40, 16, and 8 amino acid residues of AtPex3p were fused to the N terminus of the passenger protein chloramphenicol acetyltransferase (CAT) and were made as follows. Construction of pRTL2/*Sma*I-CAT with an in-frame *Sma*I site followed by the CAT coding sequence was described elsewhere [35]. PCR amplification of the 5′-120 base pairs of AtPEX3 in pU21561 included a forward primer

Table 1
N- and C-terminal amino acid sequences of *myc* epitope-tagged AtPex3p (form 2) and AtPex3p-CAT fusion proteins

Protein ID	Amino acid sequence
myc	MEGKLISEEDL
CAT	EKKIT…
n*myc*-AtPex3p	MEQKLISEEDLGSDFVRGFWRKHRRKVLVTAGCLGSGYLLYKLYNSHTRRLA…
c*myc*-AtPex3p	… NMPQEGKLISEEDL
40AtPex3p-CAT	MDFVRGRWRKHRRKVLVTAGCLGSGYLLYKLYNSHTRRLAPGEKKIT…
16AtPex3p-CAT	MDFVRGFWRKHRRKVLEKKIT…
8AtPex3p-CAT	MDGVRGFWEKKIT…
n*myc*-AtPex3p-RKHRRKΔ6G	MEQKLISEEDLGSDFVRGFW**GGGGGG**VLVTAGCLGSGYLLYKLYNSHTRRLA…
n*myc*-AtPex3p-RRKΔ3G	MEQKLISEEDLGSDFVRGFWRKH**GGG**VLVTAGCLGSGYLLYKLYNSHTRRLA…
n*myc*-AtPex3pΔTMD	MEQKLISEEDLGSDFVRGFWRKHRRKNSHTRRLA…
n*myc*-AtPex3p-F3ΔLF7ΔL	MEQKLISEEDLGSD**L**VRG**L**WRKHRRKVLVTAGCLGSGYLLYKLYNSHTRRLA…

The N-terminal most TMD1, amino acid residues 14–32 (Tmpred) is highlighted black and the cluster of basic residues is gray.

(5′-GTCCCCGGGATGGATTTCGTTAGGGGTTTTTGG-3′) that introduced an in-frame *Sma*I restriction site and a reverse primer (5′-GTCCCCCGGGAGCAAGCTACGAGTATGGGA-3′) that introduced an in-frame *Sma*I restriction site. The PCR product was TA cloned to yield pCR2.1/*Sma*I-40AtPEX3-*Sma*I. *Sma*I-digested pCR2.1/*Sma*I-40PEX3-*Sma*I was ligated into *Sma*I-digested-CIAP pRTL2/*Sma*I-CAT to yield pRTL2/40AtPEX3-CAT. Whole-plasmid PCR-based mutagenesis from pRTL2/40AtPEX3-CAT was used to generate pRTL2/16AtPEX3-CAT and pRTL2/8AtPEX3-CAT. To generate pRTL2/16AtPEX3-CAT, the PCR included a forward primer (5′-GCATAGAAGGAAGGTCTTGGAGAAAAAAATCACTGG-3′) and a reverse primer (5′-CCAGTGATTTTTTTCTCCAAGACCTTC CTTCTATGC-3′), which deleted the region of AtPEX3 coding for amino acid residues 17–40 to yield pRTL2/16AtPEX3-CAT. To generate pRTL2/8AtPEX3-CAT, the PCR included a forward primer (5′-CGTTAGGGGTTTTTGGGAGAAA AAAATCACTGG-3′) and a reverse primer (5′-CCAGTGATTTTTTTCTCCCAAAAACCCCT AACG-3′), which deleted the region of AtPEX3 coding for amino acid residues 9–40 to yield pRTL2/8AtPEX3-CAT. Constructs pRTL2/n*myc*-AtPEX3-RRKΔ3G, pRTL2/n*myc*-AtPEX3-RKHRRKΔ6G, pRTL2/n*myc*-AtPEX3ΔTMD, and pRTL2/n*myc*-AtPEX3F3ΔLF7ΔL (Table 1) were constructed using whole-plasmid PCR-based mutagenesis with pRTL2/n*myc*-AtPEX3 as template DNA. To generate pRTL2/n*myc*-AtPEX3-RRKΔ3G, the PCR included a forward primer (5′-GGAGGAAGCATGGTGGAGGGGTCTTGGTGACGGC-3′) and a reverse primer (5′-GCCGTCACCAAGACCCCTCCACCA TGCTTCCTCC-3′), which introduced nucleotide base substitutions that coded for glycine residues in place of the arginine–arginine–lysine coding sequence of AtPEX3. pRTL2/n*myc*-AtPEX3-RKHRRKΔ6G was generated via PCR using pRTL2/n*myc*-AtPEX3-RRKΔ3G as template DNA, a forward primer (5′-GTTAGGGGTTTTT GGGGTGGAGGGGGTGGAGGGGTCTTGGTGACG-3′), and a reverse primer (5′-CGTCACCAAGACCCCTCCACCCCCTCCACC CCAAAAACCCCTAAC-3′), which introduced nucleotide base substitutions coding for glycine residues in place of the argine–lysine–histidine coding sequence. To generate pRTL2/n*myc*-AtPEX3ΔTMD using pRTL2/n*myc*-AtPEX3 as template DNA, the PCR included a forward primer (5′-GGAAGCATAGAAGGAAGAATTCCCATAC TCG-3′) and a reverse primer (5′-CGAGTATGGGAATTCTTCCT TCTATGCTTCC-3′) that were designed to amplify AtPEX3 without the region coding for TMD1 (amino acid residues 14–32 were deleted [Δ]). pRTL2/n*myc*-AtPEX3F3ΔLF7ΔL was constructed using pRTL2/n*myc*-AtPEX3 as template DNA, and a forward primer (5′-GATCT GGGATCCGATCTCGTTAGGGGTCTTTGGAGGAAGCAT-3′) and a reverse primer (5′-ATGCTTCCTCCAAAGACCCCTAACG AGATCGGATCCCAGATC-3′) were included in the PCR, which introduced two point mutations in AtPEX3.

Biolistic bombardment, immunolabeling, and non-confocal epifluorescent, and laser-scanning confocal microscope analyses of Arabidopsis and BY-2 cells. Methods employed for the above procedures (techniques) have been described in detail in other papers from our laboratory [28,36,37]. Briefly, *Arabidopsis* var. Landsberg *erecta* and *Nicotiana tabacum* L., cv. Bright Yellow 2 (BY-2) suspension-cultured cells (4 days post-subculture) were transformed transiently via biolistic bombardment. Cells were harvested 2 and 5–6 h post-bombardment and fixed for 1 h in 4% (w/v) formaldehyde in *Arabidopsis* or BY-2 transformation buffer. Cell walls of both cell types were perforated and partially digested in 0.1% (w/v) Pectolyase Y-23 (Seishin Pharmaceutical, Tokyo), and *Arabidopsis* cells also were incubated in 0.1% Cellulase RS (Karlan Research Products, Santa Rosa, CA) in phosphate-buffered saline (PBS) for 2 h at 30 °C to help minimize clumping of the *Arabidopsis* cells.

Using our standard 1-mL tube method [36], cell membranes were permeabilized with 0.3% (v/v) Triton X-100 (Sigma–Aldrich) in PBS for 15 min. To determine the in vivo topology of transiently expressed *myc*-epitope-tagged AtPex3p in organellar membranes, BY-2 cells were permeabilized with digitonin, rather than with Triton X-100, following methods previously described [35,38]. Briefly, BY-2 cells (4 days post-subculture) resuspended in an equal volume of 2× growth medium (without 2,4-D) for 15 min were spread onto filter papers moistened with 2× growth medium for microprojectile bombardment. Bombarded cells were fixed and enzyme treated as describe above, and then differentially permeabilized with digitonin (25 μg/mL) (Sigma). Transformed, fixed, and permeabilized cells were incubated for 1 h each with primary and secondary antibodies in PBS following procedures described previously [35,36]. Antibody sources and concentrations used were as follows: rabbit anti-cottonseed catalase IgGs at 1:500 (v/v) or 1:1000 (v/v) (Kunce et al., 1998), mouse anti-*myc* monoclonal antibody at 1:500 (v/v) (purified 9E10, Covance, Berkeley, CA), mouse anti-CAT (chloramphenicol acetyltransferase) monoclonal antibody (undiluted culture medium) at 1:1 (v/v) (provided by S. Subramani, University of California, San Diego, CA), mouse anti-HA epitope monoclonal antibody at 1:500 (v/v) (Boehringer–Mannheim, Indianapolis, IN), mouse anti-α-tubulin monoclonal antibody 1:500 (Amersham, Arlington Heights, IL), goat anti-rabbit Cy5 at 1:500 (v/v), goat anti-rabbit rhodamine 1:1500 (v/v), and goat anti-mouse Cy2 1:500 (v/v) (Jackson Immuno Research Laboratories, Westgrove, PA).

The cells were observed and analyzed using two different microscope imaging setups. A Zeiss Axiovert 100 epifluorescence microscope (Carl Zeiss, Thornwood, NY) equipped with a CoolSnap ES CCD camera (Roper Scientific, Tucson, AZ) was used for Fig. 6. Laser confocal images were collected using a Leica DM RBE microscope equipped with Leica TCS NT scanning head (Leica, Heidelberg, Germany). All captured images were adjusted for brightness and

contrast and assembled into figures using Adobe Photoshop 6.0 (Adobe Photosystems, Klamath Fall, OR).

Results

Two putative peroxin 3 proteins in *Arabidopsis* (AtPex3p) were identified through a protein–protein BLAST (blastp) search using sequences of yeast and mammalian Pex3p homologs. The two forms were designated as forms 1 and 2. Table 2 lists all of the putative Pex3p homologs and compares their predicted molecular masses (kDa) and the percent identities of their primary amino acid sequences relative to AtPex3p forms 1 and 2. The two *Arabidopsis* forms are 72% identical. Remarkably low percent identities to form 1 and form 2 are apparent for all three known mammalian Pex3 proteins (22–25% and 19–25%, respectively) and for the four yeast Pex3 proteins (19–20% and 15–21%, respectively). Interestingly, the mammalian and yeast Pex3 proteins exhibit a relatively high degree of identity among themselves as evidenced by the narrow range (15–25%) of identity to the *Arabidopsis* Pex3p forms.

Alignments of all Pex3 proteins revealed that each possessed a cluster of basic amino acid residues within 10 residues of their N terminus. Fig. 1 shows an amino acid sequence alignment of selected portions of the N-terminal regions of the two putative *Arabidopsis* forms and the human and *Hansenula* Pex3 proteins. The latter two are included in Fig. 1 because they have the highest percent identities to the two *Arabidopsis* forms of the mammalian and yeast species. Moreover, published data are available on their putative targeting signals within the N-terminal regions of these proteins (see Discussion). All of the mammalian and plant Pex3 proteins (examples in Fig. 1) have a conserved sequence (K/R, K/R, H, K/R, K/R, and K) of six residues within the cluster that is located 8–9 residues from the N terminus. On the other hand, yeast Pex3 proteins have a recognizable, but varied, cluster of basic amino acid residues ranging 4–6 amino acid residues in length, within 4–9 residues from the N terminus. Clusters in all Pex3 proteins are nearby or adjacent to a predicted transmembrane domain (TMD). Computer programs predicted the presence of two membrane spanning helices or TMDs for both AtPex3 proteins. Fig. 1 shows that the first of two predicted TMDs, TMD1, is positioned at or near amino acid residues 14–32, and that the second TMD, TMD2, occurs at amino acid residues 121–143. Computer predictions indicate that the N terminus of

Table 2
Comparative percent amino acid identities of yeast and mammalian homologous Pex3 proteins in relation to *Arabidopsis* Pex3p forms 1 and 2

Organism	NCBI Accession	kDa	% Identity	% Identity
Arabidopsis thaliana (form 1)	NP_566598	42	100	72
Arabidopsis thaliana (form 2)	AAM70527	42	72	100
Homo sapiens	P56589	42	25	25
Mus musculus	Q9QXY9	42	22	20
Rattus norvegicus	Q9JJK4	42	22	19
Pichia pastoris	Q92262	52	20	21
Hansenula polymorpha	AAC49471	52	20	20
Yarrowia lipolytica	AA033094	48	19	19
Saccharomyces cerevisiae	NP_010616	48	19	15

```
AtPex3p1  -MDLVRGLWRKHRRKILVTTTCLGSGYLLYKLYNAHTRKLADLERELANERENDEIIKTQ 59
AtPex3p2  -MDFVRGFWRKHRRKVLVTAGCLGSGYLLYKLYNSHTRRLADLERELAHERENDEIIKTQ 59
HsPex3p   MLRSVWNFLKRHKKKCIFLGTVLGGVYILGKYGQKKIREIQERE-------AAEYIAQAR 53
HpPex3p   MFQYCRDLVSRHKKKLLFGTGVIAVSYAVSSFVSNKLAELNERLK-------EENFAKEQ 53

AtPex3p1  MKAHFDNIQMIADTTTLPHAIHHLSSRVVEEIDVSSIMDKLSKGKG-------------- 105
AtPex3p2  MKAHFESIQMIVDSTTLPHAMQFLSIRISEEIDVSHVMDRLNQGKG-------------- 105
HsPex3p   RQYHFESNQRTCNMTVLS-MLPTLREALMQQLNSESLTALLKNR---------------- 96
HpPex3p   IKRRFKQTQNDCYMTFLS-LLPVLTEPIYEALKVEEITRELQNKRFERQKAKNAPVGNST 112

AtPex3p1  -------------------------ILIPSEKLQLWNELKILSFTRMVLSLWSVTMLSLY 140
AtPex3p2  -------------------------MLSPPEKLQLWDELKILSFTRMVLSLWSVTMLSLY 140
HsPex3p   ----------------------------PSNKLEIWEDLKIISFTRSTVAVYSTCMLVVL 128
HpPex3p   DPALSTVLSDDFSVHNEKENPMHTGVQQTKSKTQLWNELRNQSITRFLTLLYCESLLIVF 172

AtPex3p1  IRVQVNILGRHLYIDTARGLGSSHL-----------LDELDLIERDDE------------ 177
AtPex3p2  IRVQVNILGRHLYVDTARALGSSHL-----------LEEVDLIDRDDE------------ 177
HsPex3p   LRVQLNIIGGYIYLDNAAVGKN---------------GTTILAPPDVQ------------ 161
HpPex3p   LHLQLNILSRRSYLETAIKLASKTKGIKLENESNVDLDPANLFLENDEELAMGSSRQDEN 232
```

Fig. 1. N-terminal sequence alignment of predicted Pex3p homologs. The *H. polymorpha* Pex3p (HpPex3p) and *Homo sapiens* Pex3p (HsPex3p) sequences were aligned with the putative *Arabidopsis* Pex3p (AtPex3p) forms 1 and 2 homologs using the ClustalW 1.82 program. The conserved clusters of basic residues highlighted in gray, and the putative TMDs in black, were predicted using TmPred (EMBnet-CH) prediction program.

the AtPex3p proteins faces the inside of an organelle/membrane compartment.

The full-length EST clone of AtPex3p (form 2) was subcloned into our plant expression vector pRTL2. The DNA encoded for an N-terminal *myc*-epitope tag (pRTL2/n*myc*-AtPEX3, Table 1) and was expressed transiently for varying times in *Arabidopsis* and BY-2 suspension-cultured cells. The subcellular localization of the gene product, n*myc*AtPex3p, was examined in both cell types using immunofluorescence microscopy. Controls such as omission and substitution of primary antibodies were included (data not shown). Figs. 2A–D and G–J show that after 2 and 5 h post-bombardment, n*myc*-AtPex3p colocalizes with endogenous peroxisomal catalase in both cell types. Peroxisomes in *Arabidopsis* cells are characteristically larger and fewer in number per cell than those in BY-2 cells [36,39]. Notably, at 2 h post-bombardment, n*myc*-AtPex3p is observed solely in peroxisomes, indicative of direct sorting to peroxisomes. Examples of an indirectly sorted protein are shown in Figs. 2E, F, K, and L. Hemagglutinin (HA) epitope-tagged peroxisomal membrane ascorbate peroxidase (HA-APX) was expressed in *Arabidopsis* and BY-2 cells. In both cell types (Figs. 2E and K), HA-APX is present in two intracellular immunofluorescent compartments, one observed as punctate structures and the other as reticular structures. Punctate HA-APX is colocalized with punctate catalase (Figs. 2F and L), whereas the reticular HA-APX is not colocalized with endogenous catalase (compare Figs. 2E with F and K with L). Taken together, these time-course results show that n*myc*-AtPex3p sorts within 2 h (the earliest time that it is detectable) directly to peroxisomes.

Fig. 3 shows the targeting of modified chloramphenicol acetyltransferase (CAT) proteins transiently expressed in *Arabidopsis* and BY-2 cells. CAT-SKL with a C-terminal serine–lysine–leucine (SKL), a prototypical type 1 peroxisomal targeting signal 1 (PTS1), was employed as a control to demonstrate targeting of a CAT protein directly to peroxisomes in both cell types. Figs. 3A, B, I, and J show a punctate colocalization in a CAT-SKL-transformed cell with endogenous catalase in both cell types. The 40 N-terminal amino acid residues of AtPex3p contain a cluster of six basic amino acid residues (RKHRRK) and the N-terminal-most TMD (TMD1) (Table 1). Figs. 3C, D, K, and L show that these 40 N-terminal amino acid residues of AtPex3p appended to the N terminus of CAT are sufficient to target CAT to peroxisomes in both cell types. Comparison of the peroxisomal images in transformed cells

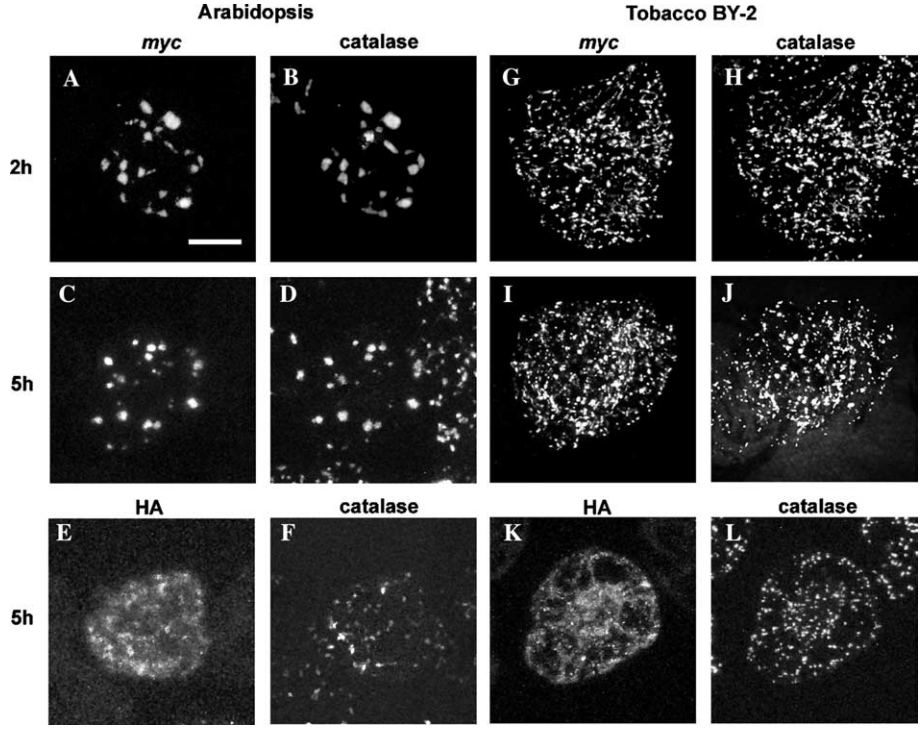

Fig. 2. Transiently expressed epitope-tagged AtPex3p (form 2) sorts directly from the cytosol to peroxisomes. *Arabidopsis* and tobacco BY-2 cells were fixed 2 or 5 h post-bombardment, permeabilized with pectolyase (and cellulase, *Arabidopsis* only) and Triton X-100, and then incubated with primary and dye-conjugated secondary antibodies. Transformed *Arabidopsis* (A–D) and BY-2 (G–J) cells were co-immunolabeled for n*myc*-AtPex3p (A,C,G,I) and endogenous peroxisomal catalase (B,D,H,J). Colocalization in peroxisomes is apparent in all cases. Transformed *Arabidopsis* (E) and BY-2 (K) cells were co-immunolabeled with hemagglutinin (HA) epitope-tagged ascorbate peroxidase (HA-APX) and catalase (F,L). Colocalization in peroxisomes is apparent and APX also is in a reticular compartment. Confocal projection micrographs. Bar = 5 μm. Confocal images (K,L) were provided by Dr. Cayle Lisenbee.

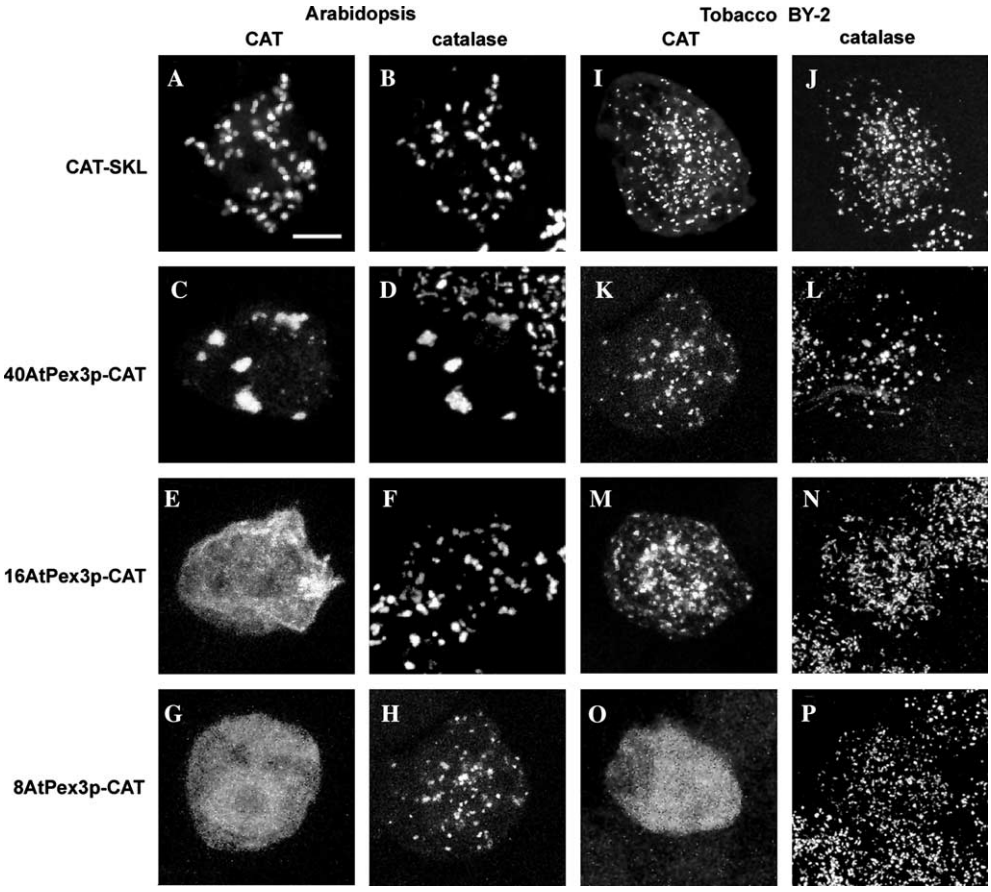

Fig. 3. The 40 N-terminal amino acid residues are sufficient to target AtPex3p chloramphenicol acetyltransferase (CAT) to peroxisomes in *Arabidopsis* and BY-2 cells. Transiently transformed (5 h) cells expressing CAT-SKL (A,I) show a colocalization with endogenous catalase in both cell types (B,J). The 40, 16, and 8 N-terminal amino acid residues of AtPex3p (form 2) were fused to CAT to yield 40AtPex3p-CAT, 16AtPex3p-CAT, and 8AtPex3p-CAT, respectively. Expression of the fusion proteins was observed in both cell types (C,E,G,K,M,O); cells were co-immunolabeled for endogenous catalase (D,F,H,L,N,P). 40AtPex3p-CAT (C,D,K,L) is colocalized in aggregated peroxisomes, whereas the other CAT fusion proteins, 16 and 8 N-terminal amino acid residues, are mislocalized to the cytosol or non-peroxisomal compartment. Confocal projection micrographs. Bar = 5 μm.

and in nearby non-transformed cells in the same picture frame (e.g., Figs. 3D and L) shows that peroxisomes in transformed cells are aggregated. Such aggregation, more pronounced in *Arabidopsis* cells, is commonly observed and has been reported previously [38].

To further define possible sufficient targeting residues of AtPex3p, the gene coding for 40AtPex3p-CAT was truncated to produce genes coding for 16AtPex3p-CAT and 8AtPex3p, which eliminated the TMD1 only and both the TMD1 and RKHRRK, respectively (Table 1). Figs. 3E, F, M, and N show that 16AtPex3p-CAT does not target to peroxisomes in either cell type. Instead, the fusion CAT protein mislocalizes to the cytosol in *Arabidopsis* cells (Fig. 3E) and to an unidentified non-peroxisomal punctate structure in BY-2 cells (Fig. 3M). The results indicate that the 8 N-terminal residues plus the RKHRRK cluster are not sufficient (without the TMD1) to target CAT to peroxisomes (Figs. 3E, F, M, and N). The fusion protein, 8AtPex3p-CAT, as expected also mislocalizes to the cytosol (Figs. 3G and O) in both cell types, indicating that the 8 N-terminal residues of AtPex3p are not sufficient for targeting CAT to peroxisomes. Note that there is no apparent aggregation of peroxisomes in *Arabidopsis* and BY-2 cells expressing 16AtPex3p-CAT or 8AtPex3p-CAT (Figs. 3F, N, H, and P, respectively). These results provide further evidence that the CAT fusion proteins did not end up in the peroxisomal membranes (see Discussion).

Fig. 4 shows subcellular localizations of altered versions of n*myc*-AtPex3p (form 2) transiently expressed in *Arabidopsis* and BY-2 cells. To ascertain the necessary role of the amino acid residues within the entire basic cluster (RKHRRK), the residues were changed to glycines (GGGGGG) and the resulting proteins (n*myc*-AtPex3p-RKHRRKΔ6G, Table 1) were expressed in both cell types (Figs. 4A and G). This mutation had the effect of n*myc*-AtPex3p-RKHRRKΔ6G mislocalizing to the cytosol in both *Arabidopsis* and BY-2 cells. To test the hypothesis that three of the six basic residues (RRK) preceding the TMD1 were essential for targeting, they

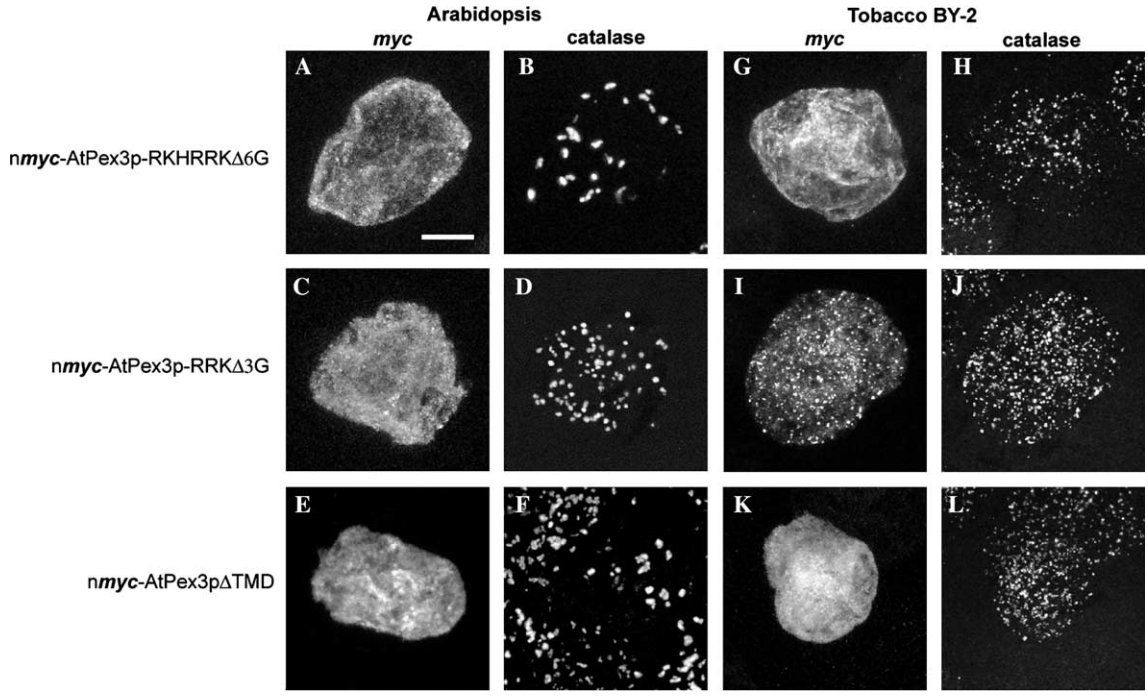

Fig. 4. An N-terminal cluster of basic amino acid residues (RKHRRK) and the adjacent TMD1 of AtPex3p (form 2) are necessary for targeting AtPex3p to peroxisomes in *Arabidopsis* (B,D,F) and BY-2 (H,J,L) cells. The transiently expressed altered versions of n*myc*-AtPex3p in both cell types are; RKHRRK and RRK residues changed to GGGGGG or GGG, and deletion of the N-terminal most TMD to yield n*myc*AtPex3p-RKHRRKΔ6G (A,G), n*myc*AtPex3p-RRKΔ3G (C,I), and n*myc*AtPex3pΔTMD (E,K), respectively. All constructs, except RRKΔ3G in BY-2 cells (I), are mislocalized to the cytosol. Confocal projection micrographs. Bar = 5 μm.

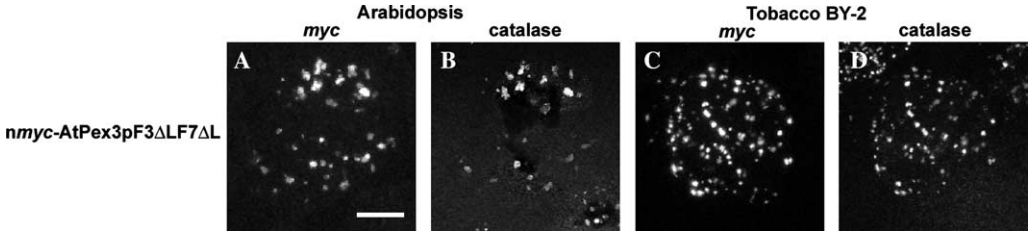

Fig. 5. The N terminus of AtPex3p (form 1) is sufficient to target the major portion of AtPex3p (form 2) to peroxisomes. Phenylalanine residues [F] at positions 3 and 7 within the N terminus of AtPex3p (form 2) were changed to leucines [L] to yield n*myc*-AtPex3pF3ΔLF7ΔL; and the proteins were expressed in *Arabidopsis* (A) and BY-2 (C) cells. This mutated construct, identical to the N terminus of form 1, colocalizes with catalase in peroxisomes (B,D). Confocal projection micrographs. Bar = 5 μm.

were changed to glycine residues and the resulting protein (n*myc*-AtPex3p-RRKΔ3G, Table 1) was expressed in both cell types (Figs. 4C and I). In *Arabidopsis* cells, n*myc*-AtPex3p-RRKΔ3G mislocalized to the cytosol (not colocalized in Figs. 4C and D), indicating that the RRK residues of RKHRRK are necessary for targeting AtPex3p (form 2) to *Arabidopsis* peroxisomes. In contrast, n*myc*-AtPex3p-RRKΔ3G in BY-2 cells sorted to peroxisomes (colocalized in Figs. 4I and J), indicating that RRK residues in this context were not necessary for targeting in BY-2 cells. To determine the necessity of TMD1 for targeting of AtPex3p to peroxisomes, transformed cells expressing n*myc*-AtPex3p (form 2) with the TMD1 deleted (n*myc*-AtPex3pΔTMD, Table 1) were examined (Figs. 4E and K). n*myc*-AtPex3pΔTMD mislocalized to the cytosol in both cell types, indicating the necessity of the TMD1 adjacent to the basic cluster of residues.

Comparisons of the amino acid residues 1–14 within the N terminus between forms 1 and 2 reveal that only two amino acid residues differ within this region (compare forms 1 and 2 in Fig. 1). To test the hypothesis that the same N-terminal 14 residues would target both AtPex3p forms to peroxisomes, the two different amino acid residues in n*myc*-AtPex3p (form 2) were mutated. Specifically, phenylalanine residues at positions three and seven in form 2 were changed to leucines to mimic the N-terminal region of AtPex3p (form 1). Figs. 5A and C shows that the resulting protein n*myc*-AtPex3pF3ΔLF7ΔL (Table 1) expresses in both

Arabidopsis and BY-2 cells and colocalizes with endogenous catalase (Figs. 5B and D). These results indicate that the N terminus of AtPex3p (form 1) is sufficient to target AtPex3p (form 2) directly to peroxisomes in both cell types.

Lee et al. [35] reported that treatment of BY-2 cells with digitonin (25 μg/mL) selectively permeabilized the plasma membrane versus the peroxisomal membrane. Our normal treatment of cells with Triton X-100 permeabilizes all cellular membranes. Fig. 6 shows BY-2 cells transiently express N- or C-terminal *myc* epitope-tagged AtPex3p (form 2) in differentially permeabilized BY-2 cells. Figs. 6A, B, G, and H illustrate transformed cells treated with Triton X-100. Both epitope-tagged versions of AtPex3p (n*myc*-AtPex3p and c*myc*-AtPex3p, Table 1) (Figs. 6A and G) are colocalized with endogenous peroxisomal catalase (Figs. 6B and H). Figs. 6C, D, I, and J show digitonin-treated cells from the same batch of bombarded cells. Fluorescence labeling attributable to n*myc*-AtPex3p (Fig. 6C), c*myc*-AtPex3p (Fig. 6I), or to endogenous catalase (Figs. 6D and J) is not observed in the cells. These results indicate that the applied anti-catalase and anti-*myc* antibodies do not reach their antigenic sites within the peroxisomal matrix because the peroxisomal boundary membranes were not detergent permeabilized. The applied antibodies reaching the cytosol outside of the peroxisomes are shown in Figs. 6E, F, K, and L. Bombarded cells treated with digitonin were co-immunolabeled for α-tubulin and peroxisomal catalase. Immunofluorescent α-tubulin in the cytoplasm is clearly observed (Figs. 6E and K), whereas peroxisomal catalase is not detected (Figs. 6F and L), indicating again that the peroxisomal membranes are not permeabilized with digitonin. These data are interpreted to indicate that the *myc*-epitope-tagged N and C termini of AtPex3p (form 2) are inaccessible to applied *myc* antibodies that reach in the cytoplasm of digitonin treated cells, thus revealing that both termini are facing the peroxisomal matrix. Taken together with the predictions that AtPex3p (forms 1 and 2) possess two TMDs within their 143 N-terminal residues (Fig. 1), it is likely that AtPex3p is anchored in the boundary

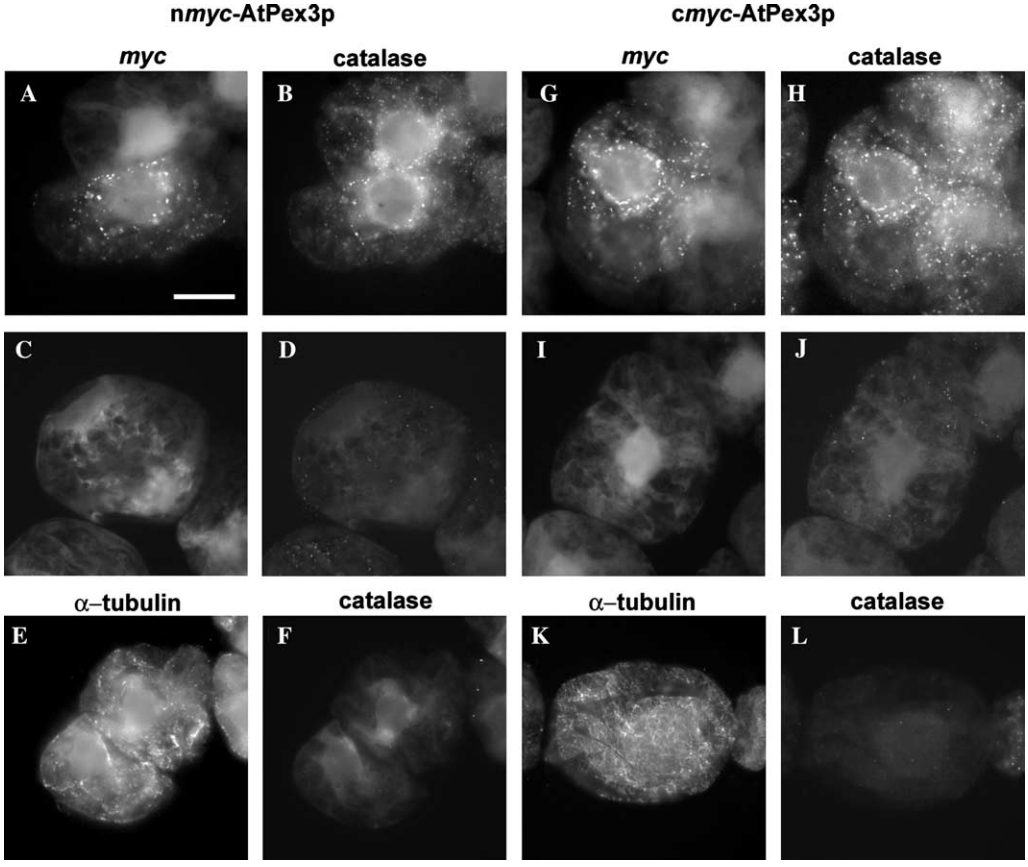

Fig. 6. The N and C termini of *Arabidopsis* Pex3p (form 2) reside within the matrix of BY-2 peroxisomes as deduced from results of in vivo differential detergent permeabilization experiments. BY-2 cells transiently expressing n*myc*-AtPex3p or c*myc*-AtPex3p were permeabilized with either Triton X-100 (A,B,G,H) or digitonin (C,D,I,J,E,F,K,L). Triton X-100-permeabilized cells were co-immunolabeled for *myc* (A,G) and endogenous peroxisomal catalase (B,H). Catalase is colocalized with n*myc*-AtPex3p and c*myc*-AtPex3p in transformed cells. Digitonin-treated transformed cells were co-immunolabeled for either *myc* (C,I) or α-tubulin (E,K) and catalase (D,F,J,L). No *myc* or catalase labeling is observed in these cells. Immunofluorescent cytosolic α-tubulin is observed in cells from the same batch of digitonin-treated cells. Non-confocal epifluorescent micrographs. Bar = 5 μm.

membrane by TMD1 with residues 33–121 facing the cytosol, and TMD2 spanning the peroxisomal membrane again such that the majority of AtPex3p and its C terminus reside in the peroxisomal matrix.

Discussion

It is well-established that peroxisomal membrane and matrix proteins are synthesized on free ribosomes and then are sorted post-translationally either directly or indirectly from the cytosol to pre-existing peroxisomes [13,21]. Sorting of PMPs via both pathways is evident in plant cells. For example, Murphy et al. [27] show in their immunofluorescence microscopy study that *Arabidopsis* PMP22 sorts directly to BY-2 cell peroxisomes. On the other hand, Mullen et al. [37,38] and Lisenbee et al. [36,39] present compelling evidence in their microscopy and cell fractionation studies that cottonseed peroxisomal APX sorts indirectly through pER to *Arabidopsis* and BY-2 cell peroxisomes.

Pex3 proteins sort to peroxisomes through different intracellular pathways depending upon the organism. For example, in several yeast species, Pex3p is reported to sort to peroxisomes via the ER. Bascom et al. [32] immunodetected overexpressed *myc*-epitope-tagged Yl-Pex3p in the ER/perinuclear regions of *Yarrowia* cells. Baerends et al. [30] showed that the 16 N-terminal amino acid residues of HpPex3p appended to a reporter protein directed this fusion protein to the ER and nuclear membranes. Similarly, Salomons et al. [40] observed accumulation of HpPex3p in the ER when *Hansenula* cells were treated with brefeldin A (BFA), which interferes with the formation of coated vesicles. In contrast, South et al. [41] found no evidence for involvement of ER in the sorting of HsPex3p to human fibroblast peroxisomes. Endogenous HsPex3p was detected only in Nycodenz-gradient isolated peroxisomes, and transiently expressed HsPex3p-*myc* was immunodetected as early as 1 h post-microinjection exclusively in peroxisomes [41].

Prior to the current study, the sorting pathway had not been elucidated for any plant putative Pex3p homolog or for any other putative peroxin homolog in plants. This statement excludes from consideration Pex5p and Pex7p, which are soluble receptor peroxins. Results of our time-course experiments indicate that n*myc*-AtPex3p sorts directly to *Arabidopsis* and BY-2 peroxisomes. At all post-bombardment time points tested, the epitope-tagged AtPex3p was observed exclusively in peroxisomes. After relatively long post-bombardment time points (e.g., 9 h), n*myc*-AtPex3p localized solely to aggregated peroxisomes (colocalized with endogenous catalase, data not shown). This observation is consistent with the localization described for overexpressed *Yarrowia lipolytica* Pex3p in clustered *Yarrowia* peroxisomes [32]. At the earliest time that n*myc*-AtPex3p could be immunodetected (2 h post-bombardment), it also was found solely in peroxisomes (Figs. 2A, B, G, and H). Peroxisomal APX (HA-epitope tagged APX) served as a positive control to show that a non-peroxisomal sorting compartment, indicative of indirect sorting, could be immuno-identified at an early stage of post-bombardment (Figs. 2E, F, K, and L). Thus, *Arabidopsis* Pex3p appears to sort directly to peroxisomes as does human Pex3p, rather than indirectly via the ER as do yeast Pex3 proteins. The definitive localization of AtPex3p (form 2) to peroxisomes within cells of two plant species (Arabidopisis and tobacco) supports our hypothesis that AtPex3p (form 2) is a plant peroxin and therefore is a homolog to the other (yeast and mammalian) Pex3 proteins.

The mPTS described herein is the only one that has been described for a plant peroxin or for any Pex3p homolog. As exemplified in Fig. 1, nearly all Pex3 proteins possess within the first 10 amino acid residues a positively charged stretch of residues in close proximity to a hydrophobic region. Kammerer et al. [33] and Ghaedi et al. [34] found that the N-terminal 40 amino acid residues of human and rat Pex3p, which included these regions, were sufficient to target GFP directly to peroxisomes. Our results are consistent with these results, i.e., the N-terminal 40 amino acid residues of AtPex3p, which also possesses both regions, are sufficient to direct a passenger protein, in our case CAT, to peroxisomes (Fig. 3). These data indicate that the mPTS for the plant and mammalian Pex3 proteins is composed of consecutive basic residues nearby a predicted TMD within the N terminus of these homologs.

Results obtained with yeast Pex3p homologs provide important data for defining the Pex3p mPTS. Weimer et al. [31] found that the 40 N-terminal amino acid residues of *Pichia* Pex3p (PpPex3p) also were sufficient to target GFP to peroxisomes, but this appended polypeptide did not possess any significant hydrophobic domain. Baerends et al. [30] reported that the 37 N-terminal amino acid residues of *Hansenula* Pex3p (HpPex3p) were sufficient to target catalase (minus its PTS, thus it served as a passenger protein) to peroxisomes; however, this polypeptide possessed a predicted TMD. Biochemical data from cell fractionation studies on HpPex3p in peroxisomal membranes provided significant insight into these apparent discrepancies. Hann et al. [42] reported that HpPex3p in peroxisomal membranes was not extracted with high salt or alkaline carbonate solutions, but was completely removed from these membranes with urea [43]. Using intact organelles, they found that the HpPex3p was digested with Proteinase K (minus detergent), indicating that HpPex3p did not possess a peroxisomal membrane spanning region(s). Thus, the question arises as to whether an authentic TMD is an essential element of the mPTS for Pex3 proteins?

Knowledge of the topological orientation of Pex3 proteins in the peroxisomal membranes is useful to help answer this question. Interestingly, the topology varies among organisms. The N terminus of ScPex3p and HsPex3p is exposed to the peroxisomal matrix with its C terminus facing the cytosol [31,33], HpPex3p is peripherally bound on the cytosolic face of the peroxisomal membrane [44], the N and C termini of RnPex3p face the cytosol [34], and both termini of AtPex3p face the peroxisomal matrix (Fig. 6). It is likely that both forms of AtPex3p possess the same topological orientation based on the identical hydropathy predictions between forms 1 and 2, and the identical sequence of amino acid residues of TMD2 within both forms.

Therefore, an authentic TMD may not constitute a necessary element of the targeting signal for all Pex3 proteins. Instead, a hydrophobic domain may be a required element of the mPTS for integral or peripheral Pex3p PMPs. Within this context, the mPTS has not been completely defined for any of the yeast or mammalian Pex3 proteins; sufficient, but not necessary, constituents have been described for a putative signal. Moreover, it is not known whether there is a separate or overlapping signal(s) for targeting of the yeast Pex3p proteins to ER (or nuclear membranes) as has been describe for ScPex15p [45] cottonseed APX [28]. The predicted TMD1 of AtPex3p (form 2) was necessary, but not sufficient, for targeting AtPex3p to peroxisomes in both cell types (Fig. 4E, F, K, and L). Our data, however, do not reveal definitively whether AtPex3p is a matrix-facing peripheral PMP or a double membrane-spanning integral PMP with its N and C termini facing the peroxisomal matrix. Nevertheless, we conclude that the N-terminal mPTS for *Arabidopsis* Pex3p (form 2, and probably form 1) is composed of three or more basic residues and an adjacent predicted/authentic TMD, which is capable of targeting the protein directly to the peroxisomal boundary membrane.

Pex3 proteins seem to function in the early stages of peroxisomal biogenesis; however, the primary role of Pex3 proteins seems to differ within yeasts and mammals. Faber et al. [46] provided evidence that HpPex3p in *Hansenula polymorpha* participates in the formation of pre-peroxisomal vesicles at the ER/perinuclear region followed by the recruitment of nascent PMPs such as Pex14p. In contrast, South et al. [41] concluded from their studies with inhibitors of COPI and COPII that HsPex3p did not associate with the ER or play any role in potential pre-peroxisomal vesiculation/origination events. Similarities between AtPex3p (form 2) and HsPex3p, such as their mPTS and direct sorting to peroxisomes, may indicate that AtPex3p does not function in pre-peroxisome membrane biosynthesis/recruitment, but functions at the peroxisomal membrane in the assembly of peroxisomal protein import machinery. The availability of appropriate *Arabidopsis* mutants will be required to test this hypothesis.

Acknowledgments

We thank Dr. Robert Mullen for constructing pRTL2/n*myc*BX and Dr. Cayle Lisenbee for providing confocal images of BY-2 HA-APX transformed cells. Special thanks are extended to Ms. Sheetal Karnik and Dr. Scott Bingham for their advice and insightful discussions on various aspects of the research. Confocal microscopic studies were performed in the ASU W.M. Keck Bioimaging Laboratory. This work was supported by NSF Grant MCB-0091826 and in part by the William and Myriam Pennington Foundation.

References

[1] F.J. Corpas, J.B. Barroso, L.A. del Rio, Peroxisomes as a source of reactive oxygen species and nitric oxide signal molecules in plant cells, Trends Plant Sci. 6 (2001) 145–150.
[2] H. van den Bosch, R.B. Schutgens, R.J. Wanders, J.M. Tager, Biochemistry of peroxisomes, Annu. Rev. Biochem. 61 (1992) 157–197.
[3] M. Veenhuis, W. Harder, Microbodies in yeasts: structure, function and biogenesis, Microbiol. Sci. 5 (1988) 347–351.
[4] G.P. Mannaerts, P.P. Van Veldhoven, Functions and organization of peroxisomal β-oxidation, Ann. NY Acad. Sci. 804 (1996) 99–115.
[5] L.M. Olivier, W. Kovacs, K. Masuda, G. Keller, S.K. Krisans, Identification of peroxisomal targeting signals in cholesterol biosynthetic enzymes: AA-CoA thiolase, HMG-CoA synthase, MPPD, and FPP synthase, J. Lipid Res. 41 (2000) 1921–1935.
[6] L.J. Olsen, J.J. Harada, Peroxisomes and their assembly in higher plants, Ann. Rev. Plant Physiol. 46 (1995) 123–146.
[7] S. Reumann, The structural properties of plant peroxisomes and their metabolic significance, Biol. Chem. 381 (2000) 639–648.
[8] P.B. Lazarow, Peroxisome biogenesis: advances and conundrums, Curr. Opin. Cell Biol. 15 (2003) 489–497.
[9] A. Baker, I.A. Graham (Eds.), Plant Peroxisomes, 1, Kluwer Academic Publishers, Dordrecht, The Netherlands, 2002.
[10] M. Hayashi, M. Nishimura, Entering a new era of research on plant peroxisomes, Curr. Opin. Plant Biol. 6 (2003) 577–582.
[11] R.T. Mullen, R.C. Flynn, R.N. Trelease, How are peroxisomes formed? The role of the endoplasmic reticulum and peroxins, Trends Plant Sci. 6 (2001) 256–261.
[12] S. Subramani, A. Koller, W.B. Snyder, Import of peroxisomal matrix and membrane proteins, Annu. Rev. Biochem. 69 (2000) 399–418.
[13] V.I. Titorenko, R.A. Rachubinski, The life cycle of the peroxisome, Nat. Rev. 2 (2001) 357–368.
[14] S. Subramani, Components involved in peroxisome import, biogenesis, proliferation, turnover, and movement, Physiol. Rev. 78 (1998) 171–188.
[15] M.R. Baumgartner, J.M. Saudubray, Peroxisomal disorders, Semin. Neonatol. 7 (2002) 85–94.
[16] R.T. Mullen, Targeting and import of matrix proteins into peroxisomes, in: A. Baker, I.A. Graham (Eds.), Plant Peroxisomes, Kluwer Academic Publishers, Dordrecht, The Netherlands, 2002, pp. 339–383.
[17] R.T. Mullen, M.S. Lee, R.C. Flynn, R.N. Trelease, Diverse amino acid residues function within the type 1 peroxisomal targeting signal, Plant Physiol. 115 (1997) 881–889.
[18] R.C. Flynn, R.T. Mullen, R.N. Trelease, Mutational analyses of a type 2 peroxisomal targeting signal that is capable of directing

oligomeric protein import into tobacco BY-2 glyoxysomes, Plant J. 16 (1998) 709–720.
[19] C. Gietl, K.N. Faber, I.J. van der Klei, M. Veenhuis, Mutational Analysis of the N-terminal topogenic signal of watermelon glyoxysomal malate dehydrogenase using the heterologous host *Hansenula polymorpha*, Proc. Natl. Acad. Sci. 91 (1994) 3151–3155.
[20] A. Kato, M. Hayashi, M. Kondo, M. Nishimura, Targeting and processing of chimeric protein with the N-terminal presequence of the precursor to glyoxysomal citrate synthase, Plant Cell 8 (1996) 1601–1611.
[21] I. Sparkes, A. Baker, Peroxisome biogenesis and protein import in plants, animals and yeasts; enigma and variations?, Mol. Membr. Biol. 19 (2002) 171–185.
[22] R.N. Trelease, Peroxisomal biogenesis and acquisition of membrane proteins, in: A. Baker, I.A. Graham (Eds.), Plant Peroxisomes, Kluwer Academic Publishers, Dordrecht, The Netherlands, 2002, pp. 305–337.
[23] J.M. Dyer, J.A. McNew, J.M. Goodman, The sorting sequence of the peroxisomal integral membrane protein PMP47 is contained within a short hydrophillic loop, J. Cell Biol. 133 (1996) 269–280.
[24] X. Wang, M.J. Unruh, J.M. Goodman, Discrete targeting signals direct PMP47 to oleate-induced peroxisomes in *Saccharomyces cerevisiae*, J. Biol. Chem. 276 (2001) 10897–10905.
[25] J.M. Jones, J.C. Morrell, S.J. Gould, Multiple distinct targeting signals in integral peroxisomal membrane proteins, J. Cell Biol. 153 (2001) 1141–1149.
[26] U. Brosius, T. Dehmel, J. Gartner, Two different targeting signals direct human peroxisomal membrane protein 22 to peroxisomes, J. Biol. Chem. 277 (2002) 774–784.
[27] M.A. Murphy, B.A. Phillipson, A. Baker, R.T. Mullen, Characterization of the targeting signal of the *Arabidopsis* 22-kDa integral peroxisomal membrane protein, Plant Physiol. 133 (2003) 813–828.
[28] R.T. Mullen, R.N. Trelease, The sorting signal for peroxisomal membrane-bound ascorbate peroxidase are within its C-terminal tail, J. Biol. Chem. 275 (2000) 16337–16344.
[29] J. Höhfeld, M. Veenhuis, W.H. Kunau, PAS3, a *Saccharomyces cerevisiae* gene encoding a peroxisomal integral membrane protein essential for peroxisome biogenesis, J. Cell Biol. 114 (1991) 1167–1178.
[30] R.J.S. Baerends, S.W. Rasmussen, R.E. Hilbrnads, M. van der Heide, K.N. Faber, P.T.W. Reuvekamp, J.A.K.W. Kiel, J.M. Cregg, I.J. van der Klei, M. Veenhuis, The *Hansenula polymorpha* PER9 gene encodes a peroxisomal membrane protein essential for peroxisome assembly and integrity, J. Biol. Chem. 271 (1996) 8887–8894.
[31] E.A.C. Wiemer, G.H. Luers, K.N. Faber, T. Wenzel, M. Veenhuis, S. Subramani, Isolation and characterization of Pas2p, a peroxisomal membrane protein essential for peroxisome biogenesis in the methylotrophic yeast *Pichia pastoris*, J. Biol. Chem. 271 (1996) 18973–18980.
[32] R.A. Bascom, H. Chan, R.A. Rachubinski, Peroxisome biogenesis occurs in an unsynchronized manner in close association with the endoplasmic reticulum in temperature-sensitive *Yarrowia lipolytica* Pex3p mutants, Mol. Biol. Cell 14 (2003) 939–957.
[33] S. Kammerer, A. Holzinger, U. Welsch, A.A. Roscher, Cloning and characterization of the gene encoding the human peroxisomal assembly protein Pex3p, FEBS Lett. 429 (1998) 53–60.
[34] K. Ghaedi, S. Tamura, K. Okumoto, Y. Matsuzono, Y. Fujiki, The peroxin Pex3p initiates membrane assembly in peroxisome biogenesis, Mol. Biol. Cell 11 (2000) 2085–2102.
[35] M.S. Lee, R.T. Mullen, R.N. Trelease, Oilseed isocitrate lyases lacking their essential type 1 peroxisomal targeting signal are piggybacked to glyoxysomes, Plant Cell 9 (1997) 185–197.
[36] C.S. Lisenbee, M. Heinze, R.N. Trelease, Peroxisomal ascorbate peroxidase resides within a subdomain of rough endoplasmic reticulum in wild-type *Arabidopsis* cells, Plant Physiol. 132 (2003) 870–882.
[37] R.T. Mullen, C.S. Lisenbee, J.A. Miernyk, R.N. Trelease, Peroxisomal membrane ascorbate peroxidase is sorted to a membranous network that resembles a subdomain of the endoplasmic reticulum, Plant Cell 11 (1999) 2167–2185.
[38] R.T. Mullen, C.S. Lisenbee, R.C. Flynn, R.N. Trelease, Stable and transient expression of chimeric peroxisomal membrane proteins induces and independent "zippering" of peroxisomes and an endoplasmic reticulum subdomain, Planta 213 (2001) 849–863.
[39] C.S. Lisenbee, S.K. Karnik, R.N. Trelease, Overexpression and mislocalization of a tail-anchored GFP redefines the identity of peroxisomal ER, Traffic 7 (2003) 491–501.
[40] F.A. Salomons, I.J. van der Klei, A.M. Kram, W. Harder, M. Veenhuis, Brefeldin A interferes with peroxisomal protein sorting in the yeast *Hansenula polymorpha*, FEBS Lett. 411 (1997) 133–139.
[41] S.T. South, K.A. Sacksteder, X. Li, Y. Liu, S.J. Gould, Inhibitors of COPI and COPII do not block *PEX3*-mediated peroxisome synthesis, J. Cell Biol. 149 (2000) 1345–1359.
[42] G.J. Haan, K.N. Faber, R.J.S. Baerends, A. Koek, A. Krikken, J.A.K.W. Kiel, I.J. van der Klei, M. Veenhuis, *Hansenula polymorpha* Pex3p is a peripheral component of the peroxisomal membrane, J. Biol. Chem. 277 (2002) 26609–26617.
[43] Y. Elgersma, L. Kwast, M. van den Berg, W.B. Snyder, B. Distel, S. Subramani, H.F. Tabak, Overexpression of Pex15p, a phosphorylated peroxisomal integral membrane protein required for peroxisome assembly in *S. cerevisiae*, causes proliferation of the endoplasmic reticulum membrane, EMBO J. (1997) 7326–7341.
[44] A.C. Muntau, P.U. Mayerhofer, B.C. Paton, S. Kammerer, A.A. Roscher, Defective peroxisome membrane synthesis due to mutations in human *PEX3* cause Zellweger syndrome, complementation group G, Am. J. Hum. Genet. 67 (2000) 967–975.
[45] R.J.S. Baerends, K.N. Faber, J.A.K.W. Kiel, I.J. van der Klei, W. Harder, M. Veenhuis, Sorting and function of peroxisomal membrane proteins, FEMS Micro. 24 (2000) 291–301.
[46] K.N. Faber, G.J. Haan, R.J.S. Baerends, A.M. Kram, M. Veenhuis, Normal peroxisome development from vesicles induced by truncated *Hansenula polymorpha* Pex3p, J. Biol. Chem. 277 (2002) 11026–11033.